

Optimization of Synthesis Conditions of $\text{LiMn}_{2-x}\text{Fe}_x\text{O}_4$ Cathode Materials Based on Thermal Characterizations

Sam Chiovoloni¹, Cristaly Moran², Peter K. LeMaire¹, Rahul Singhal^{1*}

¹Physics and Engineering Physics, Central Connecticut State University, New Britain, CT, USA

²Science, Technology, Engineering & Mathematics (STEM) Division, Naugatuck Valley Community College, Waterbury, CT, USA

Email: *singhal@ccsu.edu

How to cite this paper: Chiovoloni, S., Moran, C., LeMaire, P.K. and Singhal, R. (2017) Optimization of Synthesis Conditions of $\text{LiMn}_{2-x}\text{Fe}_x\text{O}_4$ Cathode Materials Based on Thermal Characterizations. *American Journal of Analytical Chemistry*, 8, 51-59. <http://dx.doi.org/10.4236/ajac.2017.81004>

Received: November 6, 2016

Accepted: January 8, 2017

Published: January 11, 2017

Copyright © 2017 by authors and Scientific Research Publishing Inc.

This work is licensed under the Creative Commons Attribution International License (CC BY 4.0).

<http://creativecommons.org/licenses/by/4.0/>



Open Access

Abstract

We have synthesized $\text{LiMn}_{2-x}\text{Fe}_x\text{O}_4$ ($x = 0, 0.25, \text{ and } 0.50$) cathode materials for applications in Li ion rechargeable batteries via sol-gel method. We studied thermal characteristics of as synthesized materials using differential scanning calorimetry (DSC) and thermogravimetric analysis (TGA). In order to optimize the synthesis conditions, we studied X-ray diffraction (XRD) of synthesized cathode materials at various temperatures, based on the transitions obtained from DSC/TGA. The XRD results can be co-related to the thermal behavior of the synthesized cathode materials and the synthesis conditions optimized.

Keywords

Cathode Materials, Thermal Analysis, Li Ion Rechargeable Batteries, Process Optimization, X-Ray Diffraction, Differential Scanning Calorimetry

1. Introduction

Due to technological developments and the continuous depletion of fossil fuel, the development of new power sources is of great interest. With the recent developments in the area of green energy production such as solar and wind energy, the need for high energy density energy storage devices has become equally important [1] [2] [3]. Li ion batteries have the highest energy densities among the commercially available rechargeable batteries [4] [5]. The commercially available Li ion batteries suffer from various drawbacks such as poor cyclability, rate performances and toxicity [6]. Keeping this in view, the research communi-

ty is working towards the development of new cathode materials [7] [8] [9] [10] [11]. The preparation of phase pure cathode materials for Li ion rechargeable batteries is very time consuming, since the process involves trying so many combinations of temperature and annealing time. Various authors have analyzed thermal behaviors in conjunction with X-ray diffraction (XRD), to understand the reaction mechanism for the synthesis of LiMn_2O_4 cathode materials. There is the need to continue work in this area to optimize the synthesis of these very important groups of energy storage materials.

In order to get a better understanding of the different possible by-products, Berbenni and Marini [12] studied the thermal decomposition processes taking place in solid state mixtures of $\text{Li}_2\text{CO}_3\text{-MnCO}_3$ ($x_{\text{Li}} = 0.10 - 0.50$, x_{Li} = lithium cationic fraction) in air and nitrogen flow by thermogravimetric analysis (TGA) and X-ray powder diffraction studies. They found that the formation reaction of LiMn_2O_4 and Mn_3O_4 was completed by about 720°C . At higher temperatures, complex reactions take place, resulting in the formation of the compounds $\text{Li}_2\text{Mn}_2\text{O}_4$ and LiMnO_2 with excess of Mn_3O_4 . It was also reported that in the mixture of $\text{Li}_2\text{CO}_3\text{-MnO}$, formation of LiMn_2O_4 is a two stage process, where Li_2MnO_3 forms first, followed by reaction with excess Mn_2O_3 to yield LiMn_2O_4 [13]. It has been reported that $\text{LiMn}_{1.95}\text{M}_{0.05}\text{O}_4$ ($\text{M} = \text{Al}, \text{Co}, \text{Fe}, \text{Ni}, \text{Y}$) cathode materials can be synthesized by combustion method using lithium hydroxide, manganese nitrate, M-nitrates ($\text{M} = \text{Al}, \text{Co}, \text{Fe}, \text{Ni}, \text{Y}$), and urea as precursor materials. The thermal behavior of the reaction mixture and synthesized powder revealed that the spinel phase can be achieved in 1 minute at 280°C [14].

Michalska and coworkers [15] have studied the important stages of the syntheses of nanocrystalline lithium-manganese oxide spinels using DSC-TGA measurements. They found that DSC/TGA/XRD data are co-related to each other, and all major thermal events, for all precursors occur between $500^\circ\text{C} - 700^\circ\text{C}$. The mass loss during the synthesis procedure was between 51% and 64%, depending on the material. Above 700°C pure spinel phase is obtained, as confirmed by X-ray diffraction studies.

The thermal behavior of LiMn_2O_4 spinel was studied by Molenda and coworkers [16] using DSC/TGA in the temperature range of $300^\circ\text{C} - 900^\circ\text{C}$ in air atmosphere. They reported that the changes of mass within the studied temperature range are related to arrangement of the structure accompanied by the disappearance of cations vacancies and by the formation of the stoichiometric LiMn_2O_4 . In the range of $820^\circ\text{C} - 925^\circ\text{C}$, the mass changes corresponds to the formation or disappearance of the oxygen vacancies, while above 925°C Mn_3O_4 and LiMnO_2 phases were formed and released oxygen.

In this paper, we have synthesized $\text{LiMn}_{2-x}\text{Fe}_x\text{O}_4$ ($x = 0.0, 0.25$ and 0.50) spinel cathode materials via sol-gel method. The thermal behavior of the synthesized spinel cathode materials during the calcinations process were studied using DSC/TGA. The results of thermal analysis were correlated with XRD data in order to optimize the synthesis process to obtain the phase pure materials.

2. Experimental

$\text{LiMn}_{2-x}\text{Fe}_x\text{O}_4$ cathode materials were synthesized via sol-gel method. The precursor materials lithium acetate dihydrate ($\text{LiOOCCH}_3 \cdot 2\text{H}_2\text{O}$, 99%), iron (II) acetate anhydrous ($\text{C}_4\text{H}_6\text{FeO}_4$), and Manganese(II) acetate tetrahydrate [Mn 22% (typical), $\text{C}_4\text{H}_6\text{MnO}_4 \cdot 4\text{H}_2\text{O}$] were procured from Alfa Aesar and used as received. All of the precursor materials were dissolved in 2-ethylhexanoic acid, followed by stirring for 1 hr at 500 rpm. The final solution was dried drop by drop on a Petri dish at 280°C . The resultant powders were ground and stored in a glass vial for further analysis/processing.

Simultaneous DSC/TGA measurements were carried out between 50°C and 1000°C in alumina crucibles using Q600 SDT (by TA Instruments, USA). The data were analyzed using TA Advantage software. The measurement conditions were as follows: LiMn_2O_4 (sample weight = 17 mg), $\text{LiMn}_{1.75}\text{Fe}_{0.25}\text{O}_4$ (sample weight = 25.5 mg), $\text{LiMn}_{1.5}\text{Fe}_{0.5}\text{O}_4$ (sample weight = 28.5 mg) were heated and cooled at a rate of $10^\circ\text{C}/\text{min.}$, under flow of nitrogen gas. The X-ray diffraction studies were performed using Rigaku Mini flex-II diffractometer (wavelength of X-ray, 1.5406 angstrom.) and CuK_α radiations, at a scan rate of $1^\circ/\text{min.}$ The data were collected at every 0.02° .

3. Results and Discussions

Figures 1-3 show the thermal behavior of LiMn_2O_4 , $\text{LiMn}_{1.75}\text{Fe}_{0.25}\text{O}_4$, and $\text{LiMn}_{1.5}\text{Fe}_{0.5}\text{O}_4$, respectively, obtained from DSC and TGA analysis. The XRD patterns of the synthesized materials are given in **Figures 4-6**. It can be seen from **Figures 4-6** that synthesized materials showed additional peaks, which may be due to the defects in structure. Additionally, the peaks are less intense and broader, which may be due to the lower crystallinity. Furthermore, as the calcinations temperature increases, the peaks become more sharp and intense, which may be due to the increased crystallinity. These results are in agreement as reported earlier by Molenda and coworkers [16].

It can be seen from **Figures 1-3** that there is mass loss starting at about 380°C and corresponding exothermic peak is observed. This may be due to the organic removal and removal of oxygen. **Figure 1** showed various transitions at temperatures 535°C , 665°C , 720°C , 741°C , and 781°C . The transitions between 280°C - 450°C are due to results of pyrolysis, which can be seen clearly from the peak obtained in X-ray diffraction pattern of as prepared [**Figure 4(a)**] and pyrolyzed LiMn_2O_4 [**Figure 4(b)**]. Upon further annealing at higher temperature, heat flow increases up to 705°C and corresponding mass loss is observed. This may be due to the oxygen removal from the sample and this corresponds to the decrease in peak intensity at 2 theta values of 33° , 55° , and 66° . These peaks correspond to Mn_3O_4 and Mn_2O_3 phases [13] [14]. The peak intensities corresponding to fd3m structures are increased. At 850°C , we obtained phase pure LiMn_2O_4 cathode materials. This can be verified from TGA graph [**Figure 1**], where no significant mass change is observed after 850°C .

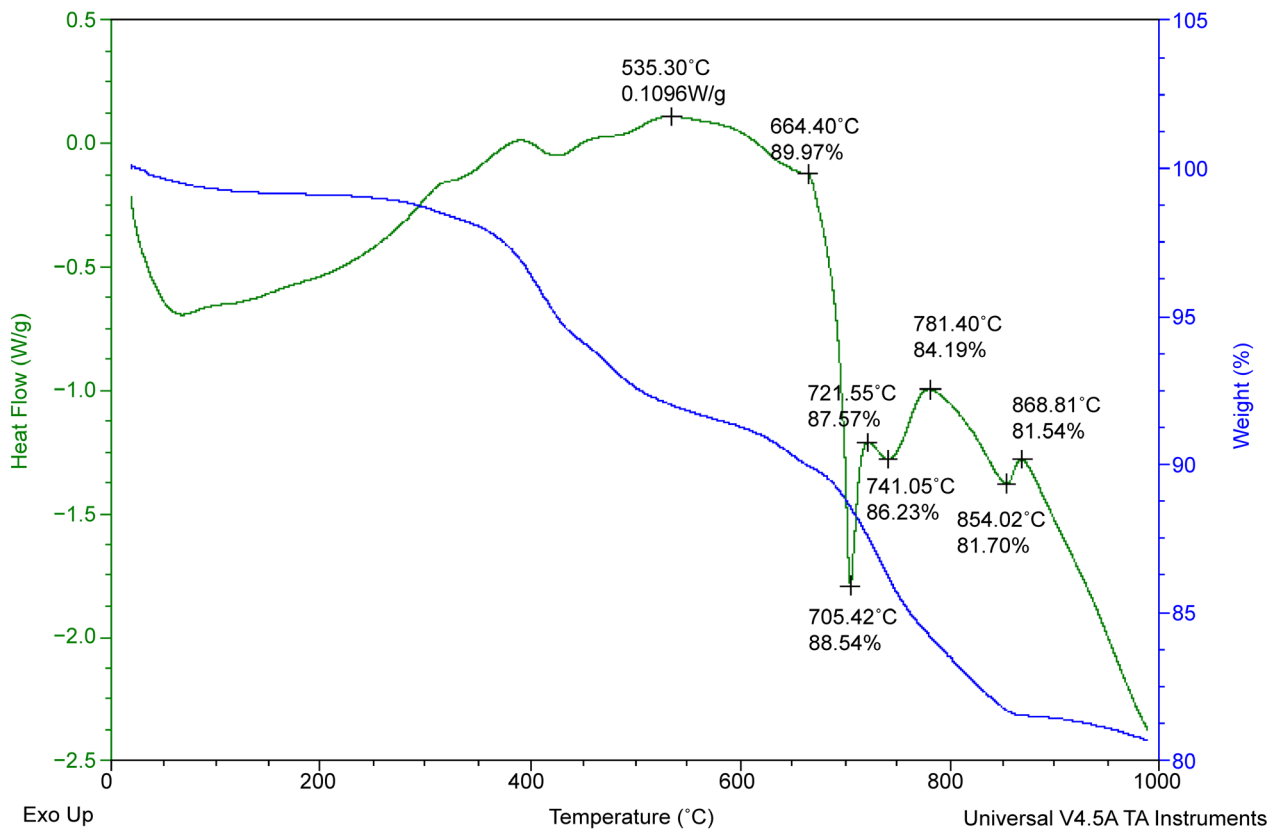


Figure 1. DSC and TGA thermograms of LiMn_2O_4 cathode materials.

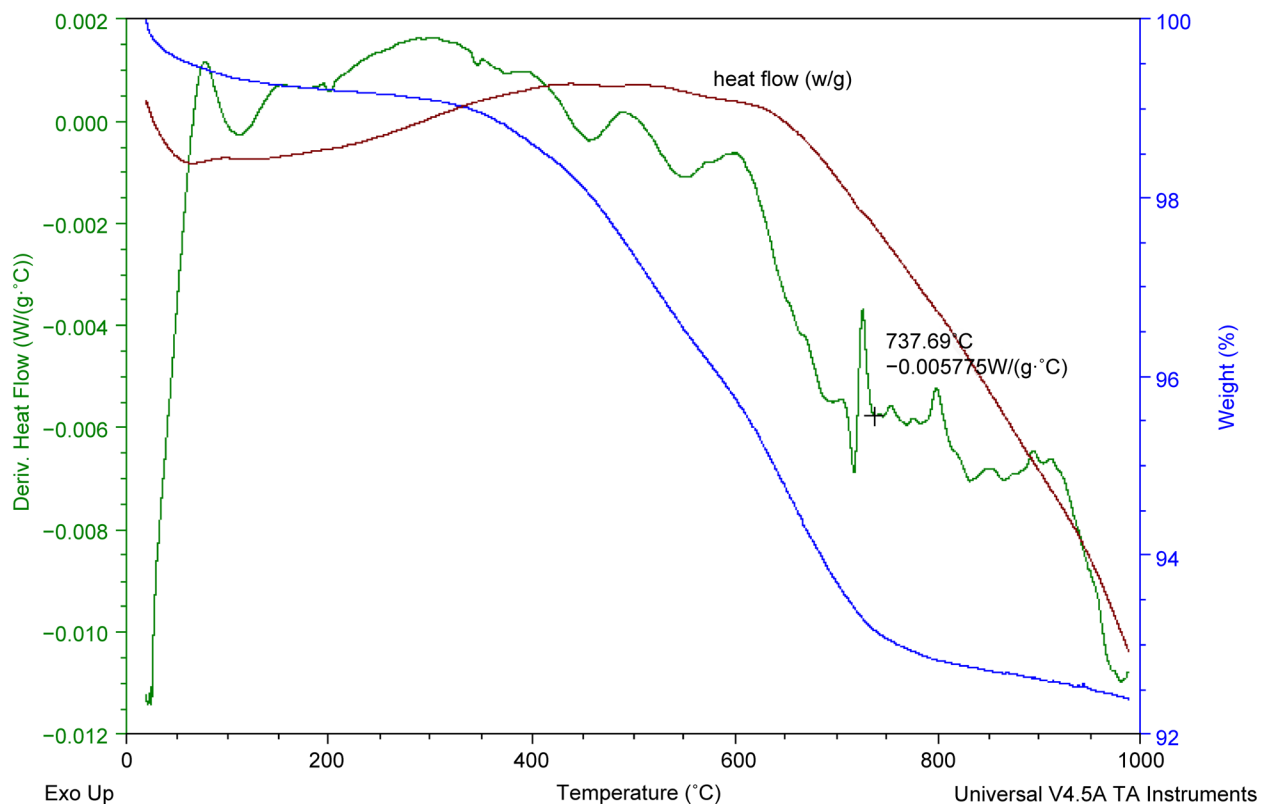


Figure 2. DSC and TGA thermograms of $\text{LiMn}_{1.75}\text{Fe}_{0.25}\text{O}_4$ cathode materials.

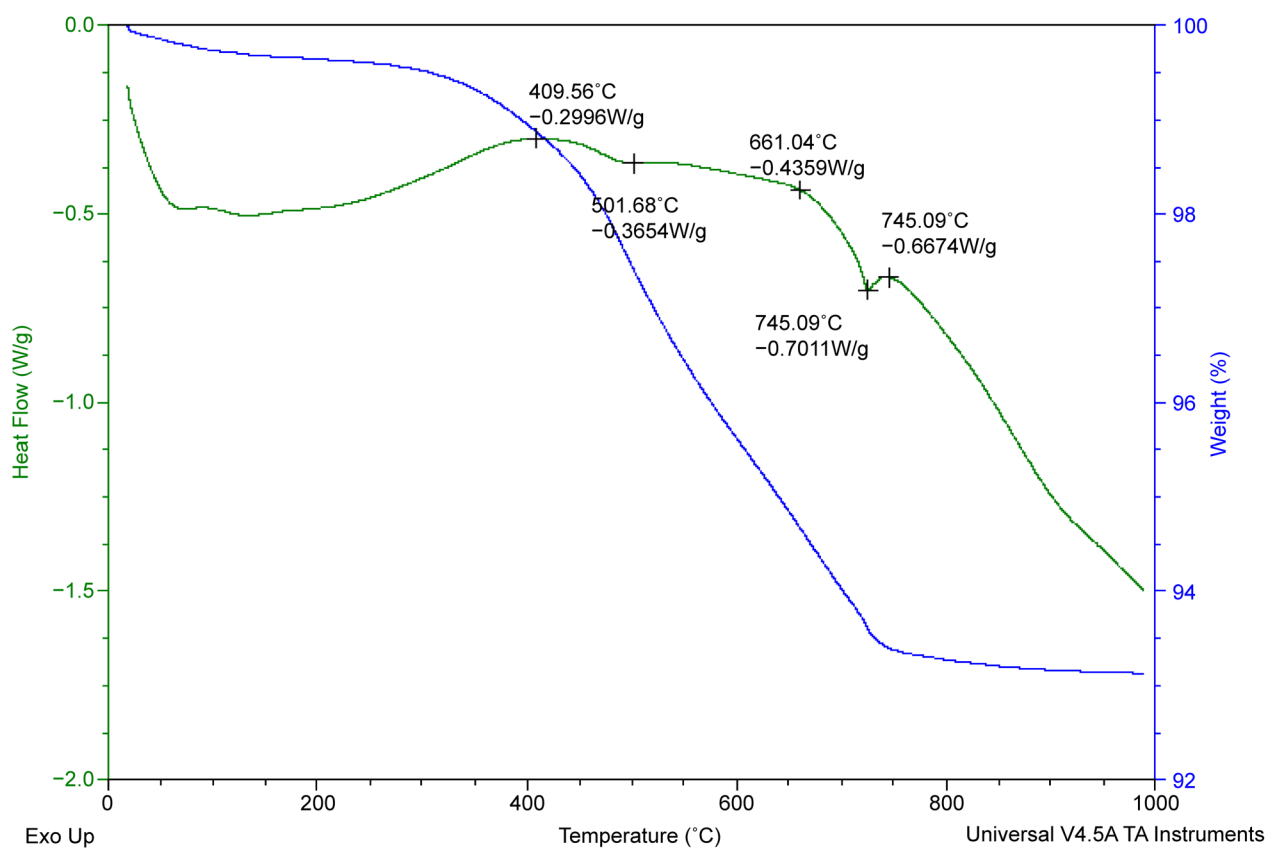


Figure 3. DSC and TGA thermograms of $\text{LiMn}_{1.5}\text{Fe}_{0.5}\text{O}_4$ cathode materials.

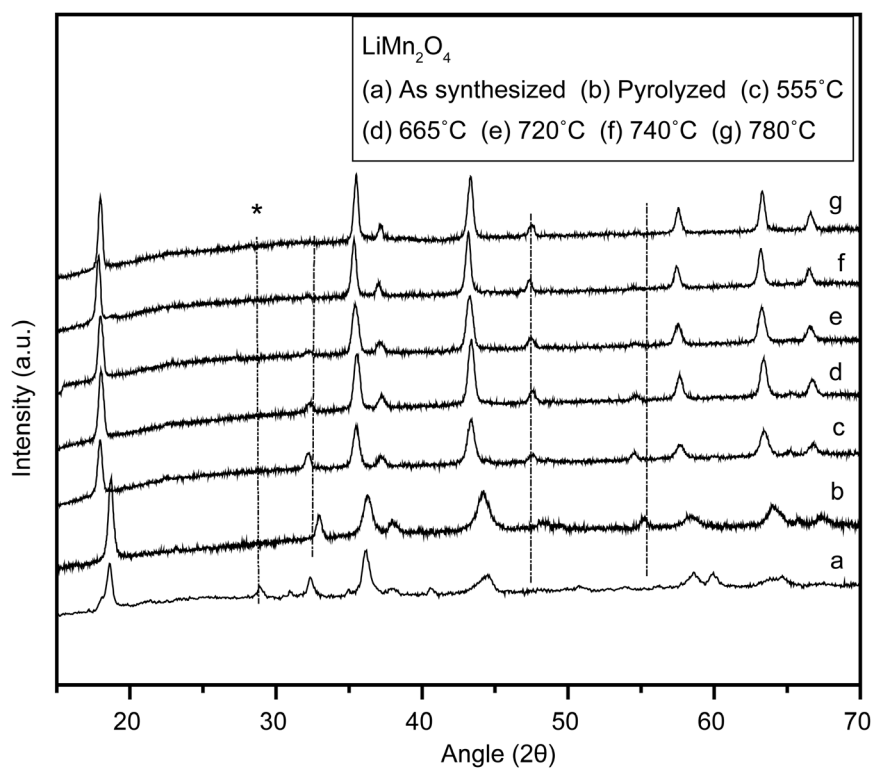


Figure 4. X-ray diffraction patterns of LiMn_2O_4 cathode materials at various calcinations temperatures.

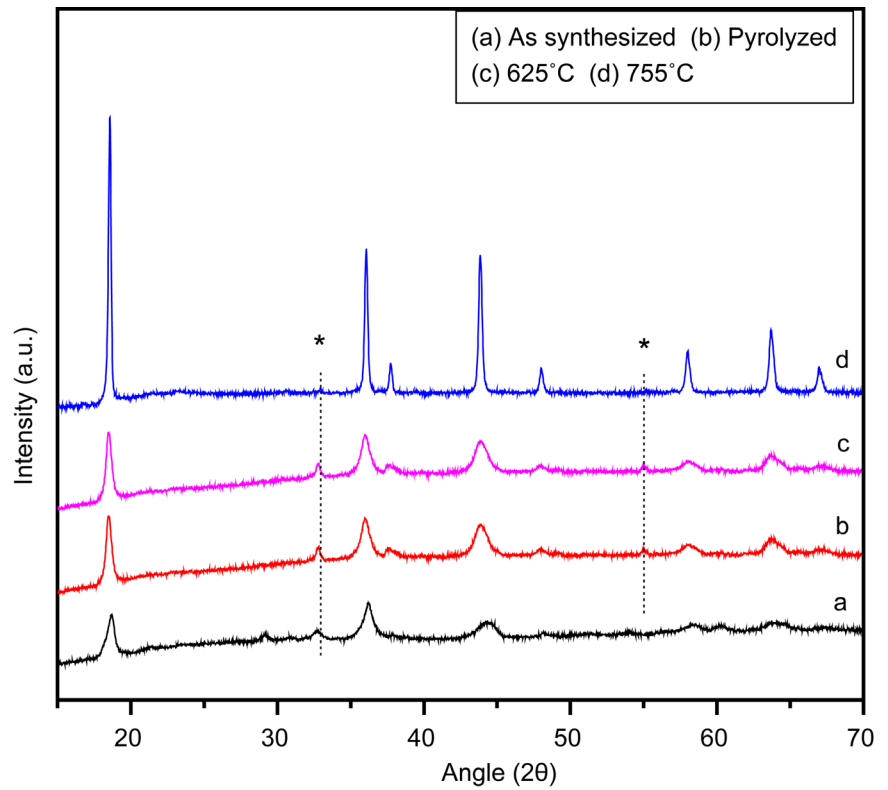


Figure 5. X-ray diffraction patterns of $\text{LiMn}_{1.75}\text{Fe}_{0.25}\text{O}_4$ cathode materials at various calcinations temperatures.

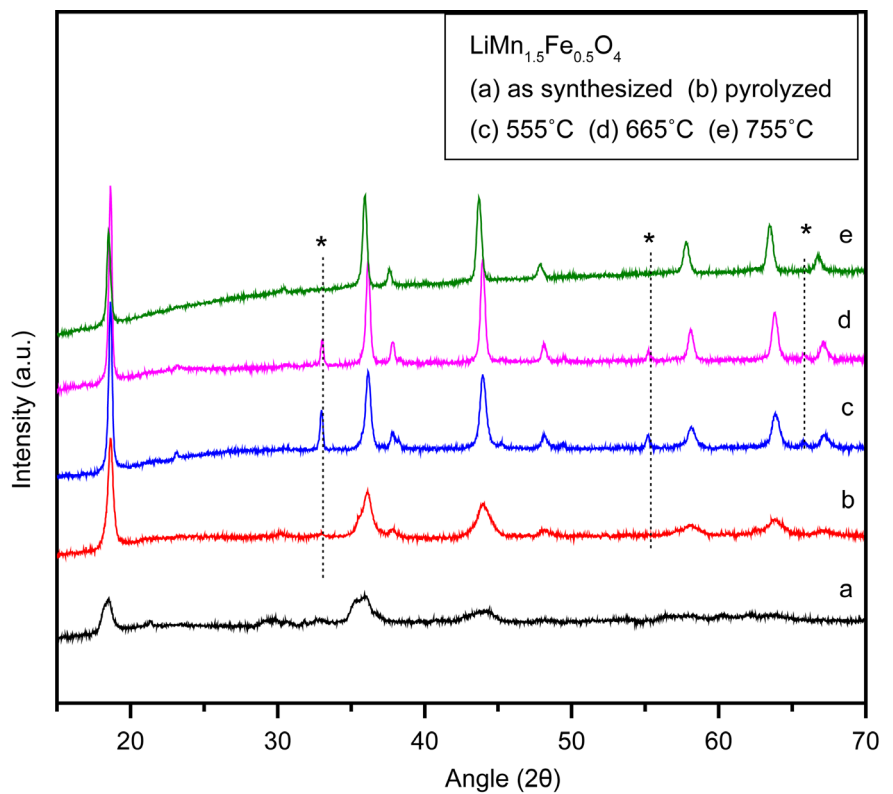


Figure 6. X-ray diffraction patterns of $\text{LiMn}_{1.5}\text{Fe}_{0.5}\text{O}_4$ cathode materials at various calcinations temperatures.

Figure 2 showed the thermal behavior of $\text{LiMn}_{1.75}\text{Fe}_{0.25}\text{O}_4$ cathode materials and corresponding XRD patterns are given in **Figure 5**. It can be seen from **Figure 2** that after pyrolysis between 200°C - 380°C , the mass decreases gradually from 380°C to 750°C , after that no significant mass loss is observed. The corresponding XRD [**Figure 5**] showed the decrease in peak intensity of peaks at 33° and 55° and increasing of spinel characteristic peaks. We obtained phase pure spinel $\text{LiMn}_{1.75}\text{Fe}_{0.25}\text{O}_4$ at 750°C , which is lower than that of pure LiMn_2O_4 cathode materials. Similar behavior was also obtained for $\text{LiMn}_{1.5}\text{Fe}_{0.5}\text{O}_4$ cathode materials, where there is mass loss up to 750°C , and after this temperature, there is no significant mass loss [**Figure 3**]. The corresponding XRD patterns of $\text{LiMn}_{1.5}\text{Fe}_{0.5}\text{O}_4$, obtained at various calcinations temperatures [as prepared, 555°C , 665°C , and 755°C] [**Figure 6**] showed that phase pure material at 755°C . **Table 1** shows the crystallite size and lattice parameters of LiMn_2O_4 , $\text{LiMn}_{1.75}\text{Fe}_{0.25}\text{O}_4$, and $\text{LiMn}_{1.5}\text{Fe}_{0.5}\text{O}_4$ cathode materials, calcined at various temperatures. It can be seen from the table that as the calcined temperature increases, lattice parameter also increases. Similar behavior was reported by Dziembaj and coworkers [17]. The crystallite size was calculated using Scherer's equation. The average crystallite sizes were found to be in the range of 13 - 40 nm. The crystallite size varies with the temperature and was found to be increased upon increasing annealing temperature. Our results are in agreement as reported earlier [18].

4. Conclusion

We have successfully synthesized spinel LiMn_2O_4 , $\text{LiMn}_{1.75}\text{Fe}_{0.25}\text{O}_4$, and $\text{LiMn}_{1.5}\text{Fe}_{0.5}\text{O}_4$ cathode materials via sol-gel method. The thermal behavior of the synthesized materials is in agreement with the results obtained from X-ray diffraction studies. Based on the results obtained from thermal and structural studies, the synthesis conditions for the cathode materials can be optimized. We obtained the optimum calcinations temperatures for LiMn_2O_4 , $\text{LiMn}_{1.75}\text{Fe}_{0.25}\text{O}_4$, and $\text{LiMn}_{1.5}\text{Fe}_{0.5}\text{O}_4$ as 850°C , 750°C , and 750°C , respectively. Further characterizations such as X-ray photoelectron spectroscopy and micro-Raman spectroscopy may be carried out to provide better understanding of the reaction mechanism.

Table 1. Lattice parameter and crystallite size of $\text{LiMn}_{2-x}\text{Fe}_x\text{O}_4$ cathode materials.

Material	Annealing temperature ($^\circ\text{C}$)	Average lattice parameter (\AA)	Average crystallite size (nm)
LiMn_2O_4	665	8.3595	20.13
	720	8.3727	19.68
	740	8.3906	27.6
	780	8.3643	25.70
$\text{LiMn}_{1.75}\text{Fe}_{0.25}\text{O}_4$	625	8.2601	12.99
	755	8.2725	39.65
$\text{LiMn}_{1.5}\text{Fe}_{0.5}\text{O}_4$	555	8.2462	26.7
	665	8.2473	22.32
	755	8.2945	23.92

Acknowledgements

The authors are thankful to Dr. Faris Malhas, Dean School of Engineering, Science and Technology, Central Connecticut State University (CCSU) for his support in the acquisition of the Q600 SDT. The financial support received from CCSU AAUP university research grant (No. ARLEMJ), and Connecticut NASA Space Grant are gratefully acknowledged.

References

- [1] Larcher, D. and Tarascon, J.-M. (2015) Towards Greener and More Sustainable Batteries for Electrical Energy Storage. *Nature Chemistry*, **7**, 19-29. <https://doi.org/10.1038/nchem.2085>
- [2] Armand, M. and Tarascon, J.-M. (2008) Building Better Batteries. *Nature*, **451**, 652-657. <https://doi.org/10.1038/451652a>
- [3] Lin, M.C., Gong, M., Lu, B., Wu, Y., Wang, D.Y., Guan, M., Angell, M., Chen, C., Yang, J., Hwang, B.J. and Dai, H. (2015) An Ultrafast Rechargeable Aluminium-Ion Battery. *Nature*, **520**, 324-328. <https://doi.org/10.1038/nature14340>
- [4] Chen, J.M., Hsu, C.H., Lin, Y.R., Hsiao, M.H. and Fey, T.K. (2008) High-Power Li-FePO₄ Cathode Materials with a Continuous Nano Carbon Network for Lithium-Ion Batteries. *Journal of Power Sources*, **184**, 498-502. <https://doi.org/10.1016/j.jpowsour.2008.04.022>
- [5] Huang, B., Shi, P.F., Liang, Z.C., Chen, M. and Guan, Y.F. (2005) Effects of Sintering on the Performance of Hydrogen Storage Alloy Electrode for High-Power Ni/MH Batteries. *Journal of Alloys and Compounds*, **394**, 303-307. <https://doi.org/10.1016/j.jallcom.2004.11.007>
- [6] Chen, Z., Lu, W.Q., Liu, J. and Amine, K. (2006) LiPF₆/LiBOB Blend Salt Electrolyte for High-Power Lithium-Ion Batteries. *Electrochimica Acta*, **51**, 3322-3326. <https://doi.org/10.1016/j.electacta.2005.09.027>
- [7] Brandt, A. and Balducci, A. (2013) Ferrocene as Precursor for Carbon-Coated α -Fe₂O₃ Nano-Particles for Rechargeable Lithium Batteries. *Journal of Power Sources*, **230**, 44-49. <https://doi.org/10.1016/j.jpowsour.2012.11.125>
- [8] Lin, Y., Lin, Y., Zhou, T., Zhao, G., Huang, Y. and Huang, Z. (2013) Enhanced Electrochemical Performances of LiFePO₄/C by Surface Modification with Sn Nanoparticles. *Journal of Power Sources*, **226**, 20-26. <https://doi.org/10.1016/j.jpowsour.2012.10.074>
- [9] Xiong, X., Wang, Z., Guo, H., Li, X., Wu, F. and Yue, P. (2012) High Performance LiV₃O₈ Cathode Materials Prepared by Spray-Drying Method. *Electrochimica Acta*, **71**, 206-212. <https://doi.org/10.1016/j.electacta.2012.03.122>
- [10] Liu, L., Lei, X., Tang, H., Zeng, R., Chen, Y. and Zhang, H. (2015) Influences of La Doping on Magnetic and Electrochemical Properties of Li₃V₂(PO₄)₃/C Cathode Materials for Lithium-Ion Batteries. *Electrochimica Acta*, **151**, 378-385. <https://doi.org/10.1016/j.electacta.2014.11.052>
- [11] Li, S., Xu, L., Li, G., Wang, M. and Zhai, Y. (2013) *In-Situ* Controllable Synthesis and Performance Investigation of Carbon-Coated Monoclinic and Hexagonal LiMnBO₃ Composites as Cathode Materials in Lithium-Ion Batteries. *Journal of Power Sources*, **236**, 54-60. <https://doi.org/10.1016/j.jpowsour.2013.02.027>
- [12] Berbenni, V. and Marini, A. (2002) Thermogravimetry and X-Ray Diffraction Study of the Thermal Decomposition Processes in Li₂CO₃-MnCO₃ Mixtures. *Journal of Analytical and Applied Pyrolysis*, **62**, 45-62.

- [https://doi.org/10.1016/S0165-2370\(00\)00211-4](https://doi.org/10.1016/S0165-2370(00)00211-4)
- [13] Berbenni, V. and Marini, A. (2002) Thermoanalytical (TGA-DSC) and High Temperature X-Ray Diffraction (HT-XRD) Study of the Thermal Decomposition Processes in $\text{Li}_2\text{CO}_3\text{-MnO}$ Mixtures. *Journal of Analytical and Applied Pyrolysis*, **64**, 43-58. [https://doi.org/10.1016/S0165-2370\(01\)00169-3](https://doi.org/10.1016/S0165-2370(01)00169-3)
- [14] Choi, H.J., Lee, K.M. and Lee, J.G. (2001) $\text{LiMn}_{1.95}\text{M}_{0.05}\text{O}_4$ (M: Al, Co, Fe, Ni, Y) Cathode Materials Prepared by Combustion Synthesis. *Journal of Power Sources*, **103**, 154-159. [https://doi.org/10.1016/S0378-7753\(01\)00835-7](https://doi.org/10.1016/S0378-7753(01)00835-7)
- [15] Michalska, M., Lipińska, L., Mirkowska, M., Aksienionek, M., Diduszko, R. and Wasiucionek, M. (2011) Nanocrystalline Lithium-Manganese Oxide Spinel for Li-Ion Batteries—Sol-Gel Synthesis and Characterization of Their Structure and Selected Physical Properties. *Solid State Ionics*, **188**, 160-164. <https://doi.org/10.1016/j.ssi.2010.12.003>
- [16] Molenda, M., Dziembaj, R., Podstawka, E. and Proniewicz, L.M. (2005) Changes in Local Structure of Lithium Manganese Spinel ($\text{Li:Mn}=1:2$) Characterised by XRD, DSC, TGA, IR, and Raman Spectroscopy. *Journal of Physics and Chemistry of Solids*, **66**, 1761-1768. <https://doi.org/10.1016/j.jpcs.2005.09.001>
- [17] Dziembaj, R., Molenda, M., Majda, D. and Walas, S. (2003) Synthesis, Thermal and Electrical Properties of $\text{Li}_{1+\delta}\text{Mn}_{2-\delta}\text{O}_4$ Prepared by a Sol-Gel Method. *Solid State Ionics*, **157**, 81-87. [https://doi.org/10.1016/S0167-2738\(02\)00192-3](https://doi.org/10.1016/S0167-2738(02)00192-3)
- [18] Park, H.B., Kim, J. and Lee, C.W. (2001) Synthesis of LiMn_2O_4 Powder by Auto-Ignited Combustion of Poly(acrylic acid)-Metal Nitrate Precursor. *Journal of Power Sources*, **92**, 124-130. [https://doi.org/10.1016/S0378-7753\(00\)00512-7](https://doi.org/10.1016/S0378-7753(00)00512-7)



Submit or recommend next manuscript to SCIRP and we will provide best service for you:

Accepting pre-submission inquiries through Email, Facebook, LinkedIn, Twitter, etc.

A wide selection of journals (inclusive of 9 subjects, more than 200 journals)

Providing 24-hour high-quality service

User-friendly online submission system

Fair and swift peer-review system

Efficient typesetting and proofreading procedure

Display of the result of downloads and visits, as well as the number of cited articles

Maximum dissemination of your research work

Submit your manuscript at: <http://papersubmission.scirp.org/>

Or contact ajac@scirp.org